Magnetic tests for magnetosome chains in Martian meteorite ALH84001

Benjamin P. Weiss*†‡, Soon Sam Kim§, Joseph L. Kirschvink*, Robert E. Kopp*, Mohan Sankaran¶, Atsuko Kobayashi‖, and Arash Komeili*

Divisions of *Geological and Planetary Sciences and ¶Chemistry and Chemical Engineering and §Jet Propulsion Laboratory, California Institute of Technology, Pasadena, CA 91125; †Department of Earth, Atmospheric and Planetary Sciences, Massachusetts Institute of Technology, Cambridge, MA 02139; and ‖Division for Human Life Technology, National Institute of Advanced Industrial Science and Technology, 1-8-31 Midorigaoka, Ikeda, Osaka 563-8577, Japan

Communicated by Norman H. Sleep, Stanford University, Stanford, CA, March 31, 2004 (received for review August 7, 2003)

Transmission electron microscopy studies have been used to argue that magnetite crystals in carbonate from Martian meteorite ALH84001 have a composition and morphology indistinguishable from that of magnetotactic bacteria. It has even been claimed from scanning electron microscopy imaging that some ALH84001 magnetite crystals are aligned in chains. Alignment of magnetosomes in chains is perhaps the most distinctive of the six crystallographic properties thought to be collectively unique to magnetofossils. Here we use three rock magnetic techniques, low-temperature cycling, the Moskowitz test, and ferromagnetic resonance, to sense the bulk composition and crystallography of millions of ALH84001 magnetite crystals. The magnetic data demonstrate that although the magnetite is unusually pure and fine-grained in a manner similar to terrestrial magnetofossils, most or all of the crystals are not arranged in chains.

A debate has been raging for the last 7 years over whether magnetite crystals in carbonate in Martian meteorite ALH84001 are four-billion-year-old fossils of magnetotactic bacteria (1–5) or are instead inorganic assemblages (6–9). Thomas-Keprta *et al.* (2–4) have identified six properties that they claim are collectively unique to magnetosomes (intracellular magnetite crystals) produced by the modern terrestrial magnetotactic bacterium strain MV-1: unusual truncated hexa-octahedral morphology, few crystallographic defects, elongated habit, narrow size distribution restricted mainly to the single domain field, high purity, and alignment in chains. From their transmission electron microscopy (TEM) analyses of individual crystals acid-extracted from ALH84001 carbonates, they have argued that some of the magnetite crystals share the first five of these properties in common with MV-1. They conclude that ≈25% of the magnetite crystals in ALH84001 zoned carbonate are most likely magnetofossils intimately mixed with a population of ≈75% inorganic magnetite. Thomas-Keprta *et al.* could not comment on the sixth property (alignment in chains) because they did not analyze the magnetite crystals *in situ*.

Friedmann *et al.* (5) have used stereo backscattered scanning electron microscopy (SEM) imaging of the surfaces of ALH84001 carbonate to argue that some of the magnetite crystals are in fact arranged in chains. If so, this would provide dramatic support for the hypothesis that the magnetite is biogenic. This is because a chain of equant magnetite crystals has higher magnetostatic energy than a ring of the crystals and is therefore not commonly observed for abiogenic magnetite in nature. Magnetosome chains are thought to be stabilized in the bacteria by a rigid biomechanical structure, because when removed from the cell they often collapse into the lower-energy ring or clumped configuration (10–12). However, the proposed chains in the images of Friedmann *et al.* (5) do not appear to be isolated from surrounding magnetite crystals, which calls into question the appropriateness of their being labeled "chains" at all rather than members of a three-dimensional clumped assemblage of crystals. Furthermore, their SEM images only barely resolve the individual crystals in the chains, and the mineralogy of those crystals is unknown.

We did not observe any isolated magnetosome chains in our previous field-emission TEM images of the magnetite and pyrrhotite assemblages in zoned ALH84001 carbonates (13). However, these and the previously discussed electron microscopy data have analyzed only a tiny fraction of the magnetite crystals in each ALH84001 carbonate [we estimate that $>10^7$ magnetite crystals are within a typical carbonate bleb (13)]. Rock magnetic techniques have the advantage of sensing the bulk properties of enormous numbers of ferromagnetic crystals at once.

Methods and Samples

We and others have recently developed several magnetic techniques capable of discerning magnetosome chains from inorganic and nonchain magnetite (14). Here we used three techniques to probe the magnetic properties of ALH84001: low-temperature cycling, the Moskowitz test, and ferromagnetic resonance (FMR).

Low-Temperature Cycling. Magnetite undergoes a phase transition at ≈125 K in which it converts from a high-temperature cubic phase to a low-temperature monoclinic phase. The actual transition temperature is depressed below this value for impure and/or partially oxidized magnetite. Magnetite will demagnetize while cooling through the Verwey transition and then recover part of its remanence upon warming back up to room temperature, with the amount recovered partly depending on the domain state (i.e., crystal size). As a result, the Verwey transition temperature is a sensitive indicator of both composition and crystal size (15). Low-temperature cycling can also be used to identify minerals other than magnetite that have magnetic transitions below room temperature. For instance, pyrrhotite has a magnetic transition at 35 K at which it will demagnetize, whereas chromite's Curie point lies between 80 K and room temperature, depending on the amount of impurities (15). To measure the low-temperature magnetism of our ALH84001 samples, we used a Quantum Designs Magnetic Property Measurement System (MPMS), a low-temperature superconducting quantum interference device (SQUID) magnetometer in the Beckman Institute at Caltech. Our low-temperature cycling protocol began with giving the sample a saturating (5 T) field at 300 K followed by quenching the field to <0.2 mT. We then cooled the sample down to 10 K and warmed it back up to 300 K, measuring its moment as a function of temperature.

Moskowitz Test. The Moskowitz test (16) is another low-temperature magnetic technique that senses the Verwey transi-

Abbreviations: TEM, transmission electron microscopy; SEM, scanning electron microscopy; FMR, ferromagnetic resonance; FC, field-cool; ZFC, zero-FC.

‡To whom correspondence should be addressed. E-mail: bweiss@gps.caltech.edu.

tion. Like low temperature cycling, the Moskowitz test gives information about the purity and, to a lesser extent, crystal size of any magnetite in the sample. Most importantly, the Moskowitz test is an indicator of the presence or absence of magnetotactic bacteria. A series of studies have argued that the test is able to identify these bacteria by means of its sensitivity both to the magnetosome chain structure (14, 16, 17) and also possibly to minor nonstoichiometry of the crystals (18, 19), both of which strongly influence the amount of demagnetization that occurs at the Verwey transition.

In the Moskowitz test, the sample is magnetized at low temperatures and then warmed up through the Verwey transition, at which point it partially demagnetizes. Following previously described protocols (14, 16), our Moskowitz test consisted of two sets of measurement suites on each sample: field-cool (FC) and zero-field-cool (ZFC). In both cases, we measured the moment of the sample as it was progressively warmed from 10 K to 300 K by using the Magnetic Property Measurement System at Caltech. FC data were taken after the sample had been cooled from 300 K to 10 K in a saturating (5.0 T) field that was then quenched to <0.2 mT at 10 K. ZFC data were taken after the sample had been cooled from 300 K to 10 K (after having quenched the magnet at 300 K); before beginning the measurements, this was followed by momentary exposure to a saturating (5.0 T) field at 10 K, which was then quenched to <0.2 mT. Following Moskowitz *et al.* (16), the splitting between the FC and ZFC curves was quantified by using the ratio δ_{FC}/δ_{ZFC} defined as $\delta_{FC,ZFC} = [M_{FC,ZFC}\ (80\ K) - M_{FC,ZFC}\ (150\ K)]/M_{FC,ZFC}\ (80\ K)$, where $M(T)$ is the moment measured at temperature T after either FC or ZFC treatment. Empirically, they found (16) that only whole cells of magnetotactic bacteria have $\delta_{FC}/\delta_{ZFC} > 2$.

FMR. FMR is primarily used as a sensor of the magnetic anisotropy fields that arise from crystal shape, composition, and mineralogy. We recently demonstrated that magnetotactic bacteria and magnetofossils with isolated intact chains of magnetite crystals have a distinct FMR spectrum by which they can be readily identified in bulk samples (14). In FMR, a sample is immersed in a dc magnetic field and exposed to microwaves. Because of the Zéeman effect, the sample can absorb this energy, with the absorption intensity depending on the strength of the applied plus any internal magnetic fields. Our FMR measurements were conducted at X-band (9.3 GHz) with the Bruker ESP 300E EPR spectrometer at the Jet Propulsion Laboratory. Most samples were analyzed at both room temperature and again at 77 K. As described previously (14), we classified the FMR spectra by using three parameters: the polycrystalline effective g factor, g_{eff}, the linewidth (ΔB and ΔB_{FWHM}), and the asymmetry ratio, A. The effective g factor is defined $g_{eff} \equiv h\upsilon/\beta B_{eff}$, where h is Planck's constant, υ is the X-band microwave frequency (9.3 GHz), β is the Bohr magneton, and B_{eff} is the applied field at which maximum absorption occurs. We define the linewidth in two different ways: as the peak-to-peak distance in the derivative spectrum (ΔB), and as the full-width at half maximum of the integrated (e.g., true absorption) spectrum (ΔB_{FWHM}) (see ref. 14). We define the asymmetry ratio as $A \equiv \Delta B_{high}/\Delta B_{low}$, where ΔB_{high} is the linewidth on the high-field side of the absorption peak (which is at B_{eff}) and ΔB_{low} is the linewidth on the low-field side of B_{eff}. Both ΔB_{high} and ΔB_{low} are half-linewidths at half maximum in the integrated spectrum. We recently showed that magnetotactic bacteria with intact chains of magnetosomes have $g_{eff} < 2.12$ and $A < 1$, and sometimes show secondary low-field absorption peaks (14). These features are present in mixed assemblages of chain and nonchain magnetite containing as little as 10% chains by mass.

Table 1. Summary of magnetic data measured on ALH84001 for this study

ALH84001 subsample	δ_{FC}	δ_{ZFC}	δ_{FC}/δ_{ZFC}	g_{eff}	ΔB, mT	A
236	0.81	0.62	1.30	2.15	101	1.07
190a	0.92	0.84	1.09	2.14	98	1.05
190b	0.75	0.61	1.24	2.13	99	1.05
Carbonate	—	—	—	2.14	99	1.05
Chromite	0.93	0.84	<1.1	—	—	—

The first three columns give the Moskowitz test parameters, and the rest of the columns give the room temperature FMR parameters (see refs. 14 and 16). For each spectrum, we report the effective g factor (g_{eff}), the peak-to-peak linewidth in the derivative spectrum (ΔB), and asymmetry ratio $A \equiv \Delta B_{high}/\Delta B_{low}$. See figure 2a of ref. 14 for a graphical depiction of these FMR parameters. The carbonate sample was too weak to be detected with the Magnetic Property Measurement System for the Moskowitz test, whereas the chromite sample was too weak to be detected with FMR at both room temperature and 77 K.

Samples. We analyzed three bulk orthopyroxenite grains with masses of 5–27 mg, an ≈100-μg chromite separate, and two separates rich in zoned carbonate from ALH84001 (Table 1). Bulk ALH84001 grains typically contain a mixture of predominantly orthopyroxene, a few percent chromite, and ≈1% magnetite (20) [of both the zoned and unzoned varieties (21)]. This composition implies that the mass of chromite present in the smallest bulk meteorite grain (190b) is ≈100 μg, which is roughly equal to the mass of the chromite separate.

Results

To measure the composition and crystal size of the magnetite, we first conducted low-temperature cycling on the two bulk ALH84001 grains. The grains undergo a Verwey transition from ≈119–122 K (Fig. 1), indicating that they contain extremely pure magnetite: $Fe_{3-x}Z_xO_4$ with $x \leq 0.01$–0.02 for a wide range of impurities Z = Zn, Ti, Al, Mg, Co, Ni, and Ga (14, 22–24). This

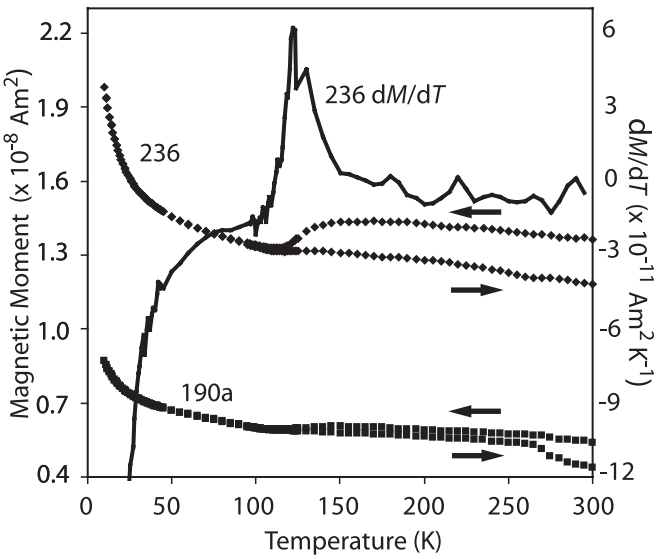

Fig. 1. Low-temperature cycling of two subsamples [236 (upper curves, ◆) and 190a (lower curves, ■)] from ALH84001 after exposure to a saturating field at 300 K. Shown is the moment of the samples in a quenched (<0.2 mT) field as they progressively cooled from 300 K to 10 K and then warmed back up to 300 K. Also shown is the computed first derivative of the moment of 236 with respect to temperature dM/dT (solid line). The peak value of dM/dT specifies the Verwey transition at 122 K for 236 and 119 K for 190a (latter derivative data not shown).

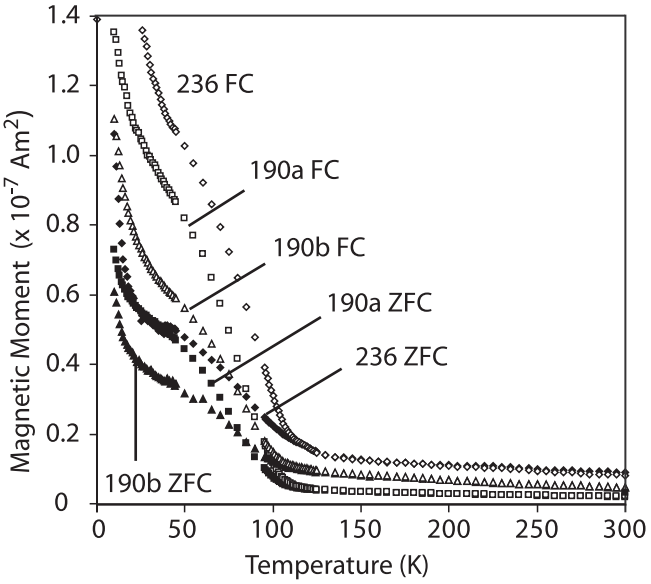

Fig. 2. Moskowitz test results on ALH84001 orthopyroxenite subsamples 236 (diamonds), 190a (squares), and 190b (triangles). Shown is the moment of the samples in a quenched (<0.2 mT) field as they progressively warmed from 10 K to 300 K after having been cooled from room temperature in a 5-T field (upper curves, open symbols) or zero field with brief 5-T pulse at 10 K (lower curves, filled symbols).

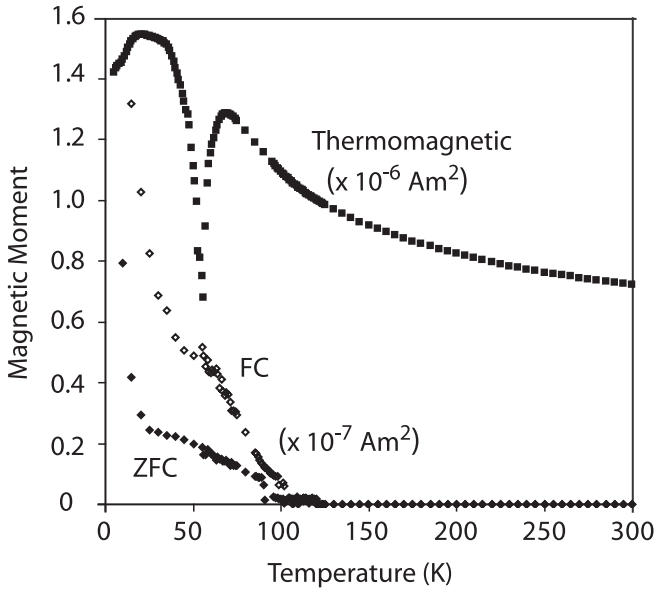

Fig. 3. Low-temperature data on ALH84001 chromite: Moskowitz test data and moment while immersed in a 5-T field. The upper and lower curves are after FC and ZFC treatments, respectively (see Fig. 2). The chromite's ≈90 K Curie point and an unusual magnetic transition at ≈55 K are marked (both reproducible in multiple measurement runs).

finding confirms and extends the conclusions of Thomas-Keprta *et al.* (2), who found that 594 individual magnetite crystals extracted from ALH84001 carbonate have $x \approx <0.01$ for each of Z = Ti, Al, Co, and Cr.

Upon warming, both bulk grains exhibited an ≈50% drop in remanence between 10 K and 298 K, but then upon warming they recovered ≈90% of their original precooling remanence (Fig. 1). This observation indicates that at room temperature ALH84001 contains a mixture of single-domain and superparamagnetic magnetite (i.e., diameters ≈<100 nm) in a roughly equal mass ratio, in qualitative agreement with previous TEM (2) and our field-emission SEM (13) data. The large decrease in remanence at ≈35 K is likely a signature of pyrrhotite (see ref. 15), which makes up 30–50% of the ferromagnetic crystals within the carbonates (the rest being magnetite) (13).

To test for chains, the bulk grains were first analyzed with the Moskowitz test (see *Methods and Samples* and refs. 14 and 16). The FC and ZFC curves split near the Verwey transition such that the bulk grains have δ_{FC}/δ_{ZFC} values between 1.1 and 1.3 (Fig. 2). The lack of additional divergence between the FC and ZFC curves at 35 K is also consistent with the presence of pyrrhotite in the grains (see ref. 25). Our low-temperature data on ALH84001 chromite confirm that it has a Curie point of ≈90 K (26),** and we find that it has $\delta_{FC}/\delta_{ZFC} < 1.1$ (Fig. 3) (upper limit because sample remanence was undetectable above ≈110 K). We can interpret our observation that all of our bulk ALH84001 grains have $\delta_{FC}/\delta_{ZFC} < 1.3$ in three ways: (*i*) there are no intact magnetosome chains in ALH84001; (*ii*) the meteorite contains a mixture of ≤40% isolated magnetosome chains with a population of nonchain magnetite (given the range of measured δ_{FC}/δ_{ZFC} and A values and comparing with ref. 16), or (*iii*) the δ_{FC}/δ_{ZFC} of the bulk grains is at least partly controlled by chromite rather than only magnetite. Because our field-emission TEM imaging (13) of an ALH84001 carbonate did not identify any isolated magnetite chains, option *ii* is highly unlikely. The low δ_{FC}/δ_{ZFC} values measured on the chromite separate do not favor, but cannot completely rule out, *iii*.

As an independent test for chains, we reanalyzed the meteorite samples with X-band FMR (see *Methods and Samples* and ref. 14). The chromite separate was apparently too small in mass to be detected with FMR both at room temperature and at 77 K, despite multiple attempts (Fig. 4). Room-temperature data on the other four samples (Fig. 4) give g_{eff}, ranging between 2.13 and

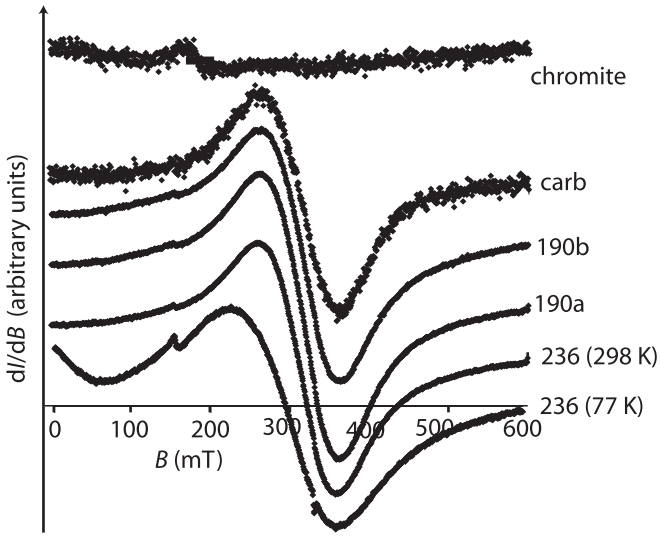

Fig. 4. Selected FMR spectra on ALH84001. Shown is the derivative of the microwave (9.3 GHz) absorption I with respect to the intensity of the applied dc field B (in arbitrary units), plotted as a function of the intensity of the field, B (in mT). The amplitude of each spectrum has been arbitrarily scaled to fit the plot. All data were taken at 298 K except for the lowermost 77 K spectrum.

**This conclusion deepens the mystery about the origin of magnetization observed in room-temperature ALH84001 chromite (13). Three possible explanations are (*i*) that the observed magnetization is an induced moment, (*ii*) that it originates from small exsolved ferromagnetic phases within the chromite, or (*iii*) that there is a subpopulation of chromites with ferromagnetic compositions distinct from the chromites analyzed here.

2.15, slightly above the g factor of stoichiometric magnetite. The samples had peak-to-peak linewidths ΔB ranging from 98 to 101 mT. FMR data on the four nonchromite samples at 77 K had $\approx$30% larger linewidths, g_{eff} shifted to $\approx$2.25, and significant zero field absorption. These differences are a reflection of magnetite's Verwey transition. Taken together, the FMR data are consistent with our field-emission TEM (13) and the above low-temperature cycling data in showing that the meteorite contains tightly clustered and magnetostatically interacting single-domain (SD) and superparamagnetic (SP) crystals. Finally, the bulk grains and carbonate samples had asymmetry ratios A = 1.03–1.07, close to that for nonchain aggregates of SD and SP magnetite. The only low-field asymmetric feature in the room-temperature spectra is a small absorption peak at $g_{\text{eff}} = 4.3$ whose intensity is inversely proportional to temperature; this peak is almost certainly from paramagnetic Fe^{3+} (27) and is not a chain signature. Clearly, the FMR data, which are not significantly influenced by the chromite, do not exhibit any evidence of isolated intact magnetosome chains.

In summary, our data confirm that ALH84001 magnetite fulfills at least two of the six criteria described by Thomas-Keprta *et al.* (2–4) as collectively unique to magnetotactic bacteria: high purity and an unusually fine-grained (single-domain to superparamagnetic) size distribution. However, our magnetic measurements, which unlike SEM reflect the bulk properties of the tens of millions of magnetite crystals in each carbonate, show that no more than $\approx$10% of the magnetite in ALH84001 can be in isolated chains. Because the chain configuration is one of the most distinctive properties of magnetosomes, our results imply it will be difficult to definitively prove that ALH84001 magnetites are magnetosome in origin. On the other hand, because in terrestrial sediments that have undergone diagenesis typically more than half of the magnetosome chain structures have been disrupted (28), our results do not rule out the claim of Thomas-Keptra *et al.* that $\approx$27% of the ALH84001 magnetite crystals are biogenic.

We thank T. Bosak for helpful advice and N. H. Sleep for communicating this manuscript. S.S.K. and the ferromagnetic resonance measurements were supported by the Mars Instrument Development Project Program; R.E.K. was supported by a National Science Foundation Graduate Research Fellowship; A. Komeili was supported by a Beckman Senior Research Fellowship; and B.P.W. and J.L.K. were supported by the National Aeronautics and Space Administration Exobiology Program and the National Aeronautics and Space Administration Astrobiology Institute.

1. McKay, D., Gibson, E., Thomas-Keprta, K., Vali, H., Romanek, C., Clemett, S., Chillier, X., Maechling, C. & Zare, R. (1996) *Science* **273,** 924–930.
2. Thomas-Keprta, K. L., Clemett, S. J., Bazylinski, D. A., Kirschvink, J. L., McKay, D. S., Wentworth, S. J., Vali, H., Gibson, E. K. & Romanek, C. S. (2002) *Appl. Environ. Microbiol.* **68,** 3663–3672.
3. Thomas-Keprta, K. L., Clemett, S. J., Bazylinski, D. A., Kirschvink, J. L., McKay, D. S., Wentworth, S. J., Vali, H., Gibson, E. K., Jr., McKay, M. F. & Romanek, C. S. (2001) *Proc. Natl. Acad. Sci. USA* **98,** 2164–2169.
4. Thomas-Keprta, K. L., Bazylinski, D. A., Kirschvink, J. L., Clemett, S. J., McKay, D. S., Wentworth, S. J., Vali, H., Gibson, E. K., Jr., & Romanek, C. S. (2000) *Geochim. Cosmochim. Acta* **64,** 4049–4081.
5. Friedmann, I. E., Wierzchos, J., Ascaso, C. & Winklhofer, M. (2001) *Proc. Natl. Acad. Sci. USA* **98,** 2176–2181.
6. Bradley, J. P., McSween, H. Y. & Harvey, R. P. (1998) *Meteorit. Planet. Sci.* **33,** 765–773.
7. Barber, D. J. & Scott, E. R. D. (2002) *Proc. Natl. Acad. Sci. USA* **99,** 6556–6561.
8. Buseck, P. R., Dunin-Borkowski, R. E., Devouard, B., Frankel, R. B., McCartney, M. R., Midgley, P. A., Posfai, M. & Weyland, M. (2001) *Proc. Natl. Acad. Sci. USA* **98,** 13490–13495.
9. Golden, D. C., Ming, D. W., Schwandt, C. S., Lauer, H. V., Socki, R. A., Morris, R. V., Lofgren, G. E. & McKay, G. A. (2001) *Am. Mineral.* **83,** 370–375.
10. Philipse, A. P. & Maas, D. (2002) *Langmuir* **18,** 9977–9984.
11. Proksch, R. & Moskowitz, B. (1994) *J. Appl. Phys.* **75,** 5894–5896.
12. Kirschvink, J. L. (1982) *Earth Planet. Sci. Lett.* **59,** 388–392.
13. Weiss, B. P., Vali, H., Baudenbacher, F. J., Kirschvink, J. L., Stewart, S. T. & Shuster, D. L. (2002) *Earth Planet. Sci. Lett.* **201,** 449–463.
14. Weiss, B. P., Kim, S. S., Kirschvink, J. L., Kopp, R. E., Sankaran, M., Kobayashi, A. & Komeili, A. (2004) *Earth Planet. Sci. Lett.*, in press.
15. Dunlop, D. J. & Ozdemir, O. (1997) *Rock Magnetism: Fundamentals and Frontiers* (Cambridge Univ. Press, New York).
16. Moskowitz, B. M., Frankel, R. B. & Bazylinski, D. A. (1993) *Earth Planet. Sci. Lett.* **120,** 283–300.
17. Carter-Stiglitz, B., Jackson, M. & Moskowitz, B. (2002) *Geophys. Res. Lett.* **29,** doi:10.1029/2001GL014197.
18. Carter-Stiglitz, B., Moskowitz, B. & Jackson, M. (2003) *Geophys. Res. Lett.* **30,** doi:10.1029/2003GL018727.
19. Carter-Stiglitz, B., Moskowitz, B. & Jackson, M. (2004) *Geophys. Res. Lett.* **31,** doi:10.1029/2003GL019155.
20. Mittlefehldt, D. W. (1994) *Meteoritics* **29,** 214–221.
21. Eiler, J. M., Valley, J. W., Graham, C. M. & Fournelle, J. (2002) *Geochim. Cosmochim. Acta* **66,** 1285–1303.
22. Muxworthy, A. R. & McClelland, E. (2000) *Geophys. J. Int.* **140,** 101–114.
23. Brabers, V. A. M., Walz, F. & Kronmuller, H. (1998) *Phys. Rev. B* **58,** 14163–14166.
24. Walz, F., Brabers, J. H. V. J. & Brabers, V. A. M. (2002) *Z. Metallkd.* **93,** 1095–1102.
25. Housen, B. A., Banerjee, S. K. & Moskowitz, B. M. (1996) *Geophys. Res. Lett.* **23,** 2843–2846.
26. Antretter, M., Fuller, M., Scott, E., Jackson, M., Moskowitz, B. & Solheid, P. (2003) *J. Geophys. Res.* **108,** doi:10.1029/2002JE001979.
27. Calas, G. (1988) in *Spectroscopic Methods in Mineralogy and Geology*, ed. Hawthorne, F. C. (Mineral. Assoc. Am., Washington, DC), pp. 513–571.
28. McNeill, D. F. & Kirschvink, J. L. (1993) *J. Geophys. Res.* **98,** 7977–7986.